TECHNIQUES *by M. Ragulskis and L. Ragulskis*

ON INTERPRETATION OF FRINGE PATTERNS PRODUCED BY TIME AVERAGE PHOTOELASTICITY

Photoelasticity[1,2] is a classical optical technique for static stress analysis. Time average photoelasticity would be of interest in some application areas. The subject of the current analysis is not dynamic photoelasticity[3] where a set of slides is photographed during the dynamic process. It is time average photoelasticity where one picture is formed averaging over the whole dynamic process. An example of potential application could be in ultrasonic motors[4] where the interaction between elastic vibrating elements plays a key role in the dynamic behavior of the system. Stroboscopic illumination[1] can be used for photoelastic analysis of vibrating components. An alternative technique to stroboscopic illumination is the time averaging procedure which could be used for direct interpretation of time averaged patterns of photoelastic fringes. As viscoelastic material behavior can take place at higher frequencies of oscillation, such effects need to be evaluated.

It is quite natural to expect that fringe interpretation produced by optical methods based on time averaging techniques will differ from the ones based on static techniques. Principal differences between time average and double exposure laser holography,[1] time average and static geometric moiré[5] could be mentioned. In time average photoelasticity, how can the generated fringe patterns be interpreted? The answer to that question is sought exploiting analytical and validated numerical techniques[6] mimicking optical experimental results in a virtual digital environment.

THEORETICAL ANALYSIS

Principal stresses σ_1, σ_2 and the directions of the principal stresses $\{V_1\}$, $\{V_2\}$ at any point of the analysed structure are calculated from FEM results[7] as eigenvalues and normalized eigenvectors of the following matrix:

$$\begin{bmatrix} \sigma_x & \tau_{xy} \\ \tau_{xy} & \sigma_y \end{bmatrix} \tag{1}$$

where σ_x, σ_y and τ_{xy} are the components of the stresses in the problem of plane stress. Then the intensity in the photoelastic image of the plane polariscope (isoclinics and isochromatics intertwined) is calculated as:[8]

$$I_1 = 4((\{V_1\} \cdot \{P\})(\{V_2\} \cdot \{P\})\sin(C(\sigma_1 - \sigma_2)))^2 \tag{2}$$

where $\{P\}$ is the vector of polarization and C is a positive constant dependent on the thickness of the analyzed structure in the state of plane stress and on the material from which it is produced.[8] It can be noted that the intensity is a continuous function in the range from 0 to 1 where 0 corresponds to black color (dark zone) and 1 corresponds to white color (bright zone). Intermediate values of intensity correspond to greyscale colors.

M. Ragulskis is a Professor in the Department of Mathematical Research Systems at Kaunas University of Technology, Kaunas, Lithuania. L. Ragulskis is a Research Associate at Vytautas Magnus University, Kaunas, Lithuania.

The intensity of the photoelastic image for the circular polariscope (isochromatics) is calculated as:[8]

$$I_2 = (\sin(C(\sigma_1 - \sigma_2)))^2 \tag{3}$$

Now we assume that the analyzed structure performs harmonic vibrations around the status of equilibrium. Stresses σ_x, σ_y and τ_{xy} will oscillate in time, and thus the principal stresses will oscillate in time too due to the linearity of the eigenvalue problem, while the directions of principal stresses will be constant. Without loss of generality we analyze isochromatics (image of the circular polariscope) only. Then the time averaged pattern of isochromatics becomes:

$$\begin{aligned} I_T &= \lim_{T\to\infty} \frac{1}{T} \int_0^T (\sin(C(\sigma_1 - \sigma_2)\sin(\omega t)))^2 \, dt \\ &= \frac{1}{2} - \frac{1}{2} \lim_{T\to\infty} \frac{1}{T} \int_0^T (\cos(2C(\sigma_1 - \sigma_2)\sin(\omega t)))dt \\ &= \frac{1}{2} - \frac{1}{2} \lim_{T\to\infty} \frac{1}{T} \left(\int_0^T (\cos(2C(\sigma_1 - \sigma_2)\sin(\omega t)))dt \right. \\ &\quad \left. + j \int_0^T (\sin(2C(\sigma_1 - \sigma_2)\sin(\omega t)))dt \right) \\ &= \frac{1}{2} - \frac{1}{2} \lim_{T\to\infty} \frac{1}{T} \int_0^T \exp j(2C(\sigma_1 - \sigma_2)\sin(\omega t))dt \\ &= \frac{1}{2} - \frac{1}{2} J_0(2C|\sigma_1 - \sigma_2|) \end{aligned} \tag{4}$$

where t is time variable, T is time of exposure, ω is angular frequency, j is imaginary unit, J_0 is the zeroth order Bessel function of the first kind. The last transition in the previous equation is possible due to the unevenness of the sine function (in the imaginary part of the integral). The relationships between the intensity of illumination and the argument $C(\sigma_1 - \sigma_2)$ for static and time average photoelasticity are presented in Fig. 1.

Interesting is the fact that the roots of equations $I_2 = 0.5$ and $I_T = 0.5$ almost coincide with a certain shift. This is a quite unexpected result, keeping in mind that the density of fringes in double exposure and time average pictures is quite different for other optical techniques (laser holography, geometric moiré).

The roots of the equation $I_2 = 0.5$ are:

ON INTERPRETATION OF FRINGE PATTERNS

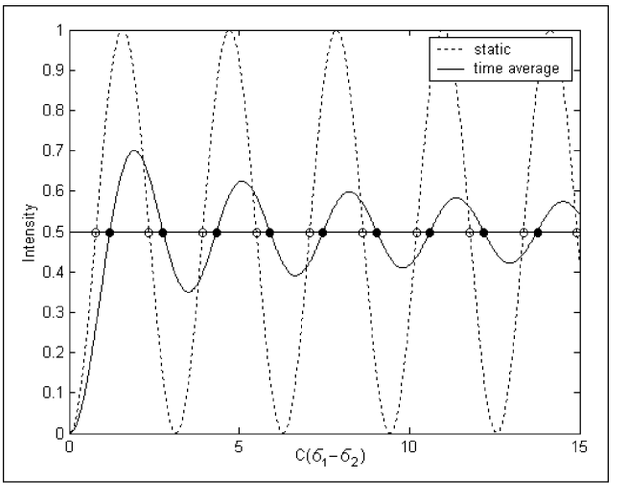

Fig. 1: Relationships between intensity and the difference between principal stresses

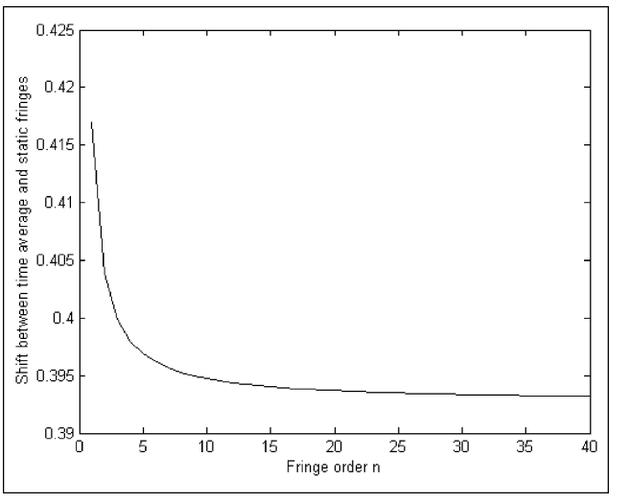

Fig. 2: Shift between time average and static fringes versus fringe order

$$C(\sigma_1 - \sigma_2) = \frac{\pi}{4} + \frac{\pi}{2} k,\ k \in Z \tag{5}$$

The roots of the equation $I_T = 0.5$ coincide with the roots of the equation

$$J_0(2C|\sigma_1 - \sigma_2|) = 0 \tag{6}$$

The roots of the zeroth order Bessel function of the first kind r_n, $n \in N$ are available in classical texts.[9] Thus, the value of the shift between the roots of the equations $I_2 = 0.5$ and $I_T = 0.5$ can be explicitly defined as:

$$\frac{r_n}{2} - \left(\frac{\pi}{4} + (n - 1)\frac{\pi}{2}\right),\ n \in Z \tag{7}$$

The term $(n - 1)$ in Eq. 7 should not confuse—the first half intensity level of the fringe for the static image corresponds to $C(\sigma_1 - \sigma_2) = \frac{\pi}{4}$ at $k = 0$ (Fig. 1), but the first half intensity level of the fringe for the time average image corresponds to $\frac{r_1}{2}$. This shift is to be taken into account when an accurate comparison between the results from static and time average analyses is performed. Keeping in mind that the Bessel function is not periodic, the variation of the shift with respect to the fringe order is presented in Fig. 2. It can be noted that the shift monotonically decreases to a certain positive value.

The presented analysis is valid not only for quasistatic harmonic motion at low frequency of excitation, but also for the resonance vibrations according to the eigenmode. In this case the dynamics of the system is described by the matrix differential equation $[M]\{\ddot{\delta}\} + [C]\{\dot{\delta}\} + [K]\{\delta\} = \{F(t)\}$, where $[M]$, $[C]$, $[K]$ are mass, viscous damping and stiffness matrixes; $\{\delta\}$, $\{F(t)\}$ are vectors of generalized nodal displacements and loading; the upper dot denotes differentiation with respect to time t. The damping matrix is usually expressed as $[C] = \alpha[M] + \beta[K]$, where α, β are the coefficients of external and internal damping.[7] Modal decomposition of the solution produces $\{\delta\} = [\{\delta_1\}\ \{\delta_2\}\ \ldots]\begin{Bmatrix} z_1 \\ z_2 \\ \vdots \end{Bmatrix} = [\Delta]\{z\}$, where $\{\delta_i\}$ is the i-th eigenmode; z_i is the i-th modal decomposition coefficient; $[\Delta]$ is the matrix of the eigenmodes; $\{z\}$ is the vector of modal coefficients. Then the modal equations take the form $\ddot{z}_i + 2\omega_i c_i \dot{z}_i + \omega_i^2 z_i = \{\delta_i\}^T\{F\}$, where ω_i is the i-th eigenfrequency of the undamped system; $c_i = \frac{1}{2}\left(\frac{\alpha}{\omega_i} + \beta\omega_i\right)$. By assuming harmonic single phase excitation $\{F(t)\} = \{F^s\}\sin \omega t$, where ω is the frequency of excitation; $\{F^s\}$ is the excitation amplitude vector. Then the steady state motion can be expressed as $z_i = z_i^s \sin \omega t + z_i^c \cos \omega t$, where z_i^s, z_i^c are the amplitudes of the sine and cosine components of the modal decomposition coefficient.

Further, the frequency of excitation is selected near to the eigenfrequency of a certain eigenmode. Then it can be assumed that the motion takes place according to a single eigenmode and the structure performs harmonic vibrations with the same phase. In this case the influence of viscous damping affects only the amplitude of motion. Then the stroboscopic photoelastic image (corresponding to the state of maximum deflection according to the eigenmode) can be compared with the time average photoelastic image using the previously described technique.

In the case when linear viscoelastic properties of the material are to be taken into account, the modal decomposition of the solution (utilizing the eigenpairs of the corresponding elastic body) can be performed similarly as for the case of viscous damping.[10] In this problem the steady state variation of displacements and stresses is also harmonic while their amplitudes and phases are determined by the sine and cosine Fourier transforms of the kernel of integral equations describing stress history in viscoelastic material.[10] Thus the stroboscopic and time averaged images can be compared in

the same way as for the case of viscous damping (under the assumption of the single mode excitation).

In the case when nonlinear viscoelastic properties[11] of the material are to be taken into account, the variation of the displacements and stresses is not necessarily harmonic and the described approach is not applicable. This is true for other types of nonlinear behavior such as plasticity or viscoplasticity.

NUMERICAL RESULTS

A rectangular, cantilevered plate with fixed lower and upper edges, in a state of plane stress is analyzed (Fig. 3a). Both edges of the plate are fastened (both components of displacements are assumed equal to zero). It is assumed that the upper edge is kinematically pressed with constant load. A numerically constructed image of smoothed isochromatics produced from FEM calculations is presented in Fig. 3a. The numerical procedures of constructing photoelastic images on the basis of numerical calculations are described in detail in reference.[8]

The numerically constructed image in Fig. 3b shows the same plate but with harmonic kinematic excitation of the upper edge when the amplitude of oscillations corresponds to static kinematic displacement in Fig. 3a. The frequency of excitation is several times lower than the first eigenfrequency (quasistatic motion is analyzed). The image of time average isochromatics (circular polariscope) is of decreased contrast due to the decay of the Bessel function at higher values of the argument. Nevertheless the fringes are clearly interpretable. Digital image brightening techniques[6] required in time average holographic image analysis can be avoided due to the fact that the value of I_T tends to 0.5—grey color (instead of 0—black color—in time average holography) at increasing argument.

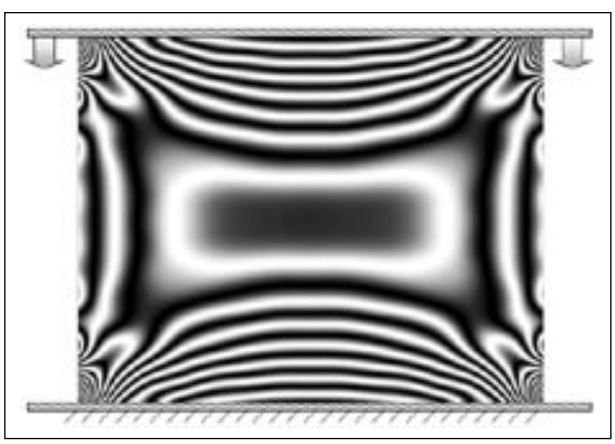

Fig. 3a: Isochromatics for static photoelasticity

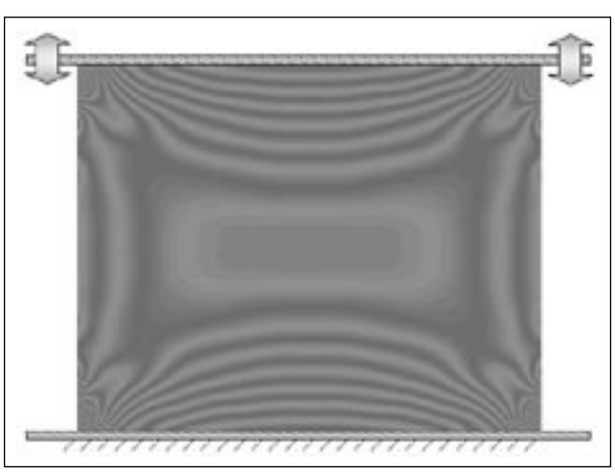

Fig. 3b: Time average isochromatics

Alternatively, the same plate with motionlessly fixed upper and lower edges is analyzed when performing harmonic vibrations according to the first eigenmode. Figure 4a presents the stroboscopic photoelastic image for a plane polariscope when the angle of polarization is $\frac{\pi}{8}$. The corresponding time average image is presented in Fig. 4b.

CONCLUSIONS

The presented technique of interpretation of time average photoelastic images is not trivial. The photoelastic image is black when the object is in a state of equilibrium and the stresses are zeroes. The pattern of isochromatics changes dynamically when the object (and stresses) oscillate in time. Nevertheless, a pattern of fringes is formed in the process of time averaging, though the contrast of the picture is decreased. The density of the fringes in the time average pattern practically coincides with the static pattern at maximum stresses. Therefore, maximum stresses in the process of vibration can be evaluated from time average isochromatics using standard fringe counting techniques,—which is an unexpected result.

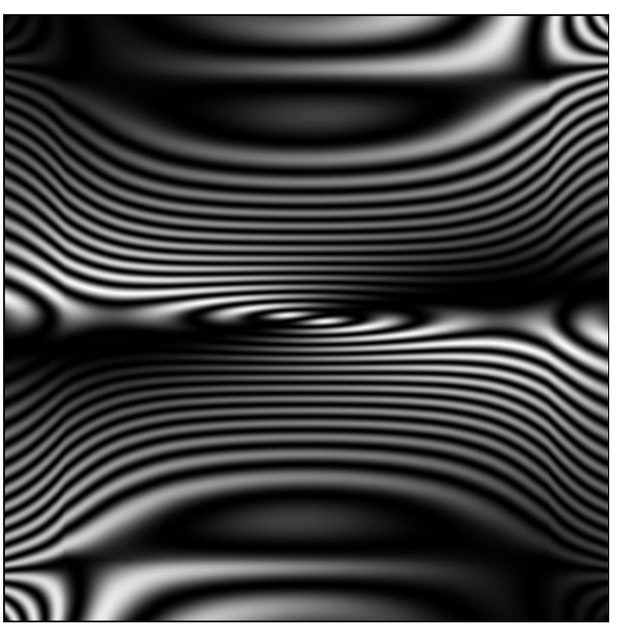

Fig. 4a: Stroboscopic image of the plane polariscope

ON INTERPRETATION OF FRINGE PATTERNS

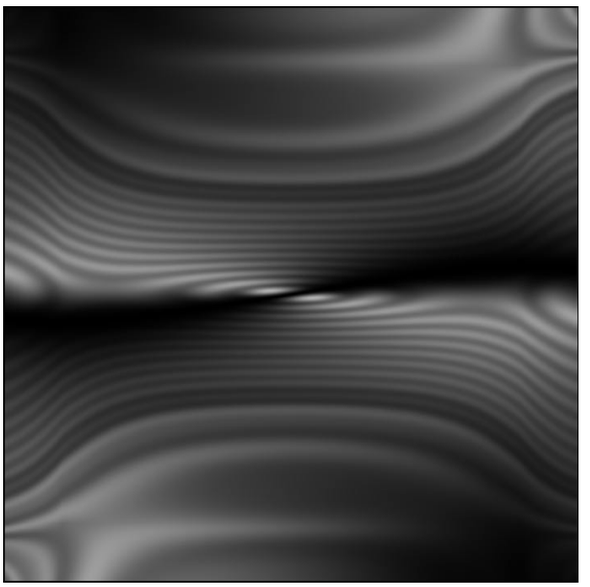

Fig. 4b: Time average image of the plane polariscope

Comparisons between stroboscopic and time average images are analyzed when the birefringent object is excited at higher frequencies. These are common if the objects are excited at resonant frequencies. Then the same technique for image comparison is valid when linear viscoelastic behavior takes place.

References

1. Handbook on Experimental Mechanics, Second Edition. Ed. A.S. Kobayashi. SEM, 1993.

2. Dally, J.W., Riley, W.F., Experimental Stress Analysis, McGraw Hill Book Company, New York, 1991.

3. Asundi, A., Sajan, M.R., "Multiple LED Camera for Dynamic Photoelasticity", Applied Optics, Vol. 34, No. 13, p.p. 2236–2240, 1995.

4. Ragulskis, K., Bansevicius, R., Barauskas, R., Kulvietis, G., Vibromotors for Precision Microrobots, New York, Hemisphere, 1987.

5. Ragulskis, M., Ragulskis, L., Maskeliunas, R., "Applicability of Time Average Geometric Moire for Vibrating Elastic Structures", Experimental Techniques, Vol. 28, No. 4, p.p. 27–30, 2004.

6. Ragulskis, M., Palevicius, A., Ragulskis, L., "Plotting Holographic Interferograms for Visualisation of Dynamic Results from Finite Element Calculations", International Journal for Numerical Methods in Engineering, Vol. 56, No. 11, p.p. 1647–1659, 2003.

7. Bathe, K.J., Finite Element Procedures in Engineering Analysis, Prentice-Hall, New Jersey, 1982.

8. Ragulskis, M., Ragulskis, L., "Plotting Isoclinics for Hybrid Photoelasticity and FEM Analysis", Experimental Mechanics, Vol. 44, No. 3, p.p. 235–240, 2004.

9. Vest, C.M., Holographic Interferometry, New York, Wiley, 1979.

10. Koltunov, M.A., Kravchuk, A.S., Majboroda, V.P., Applied Mechanics of Deformable Solid Body, Vysshaja Shkola, Moscow, 1983.

11. Yoneyama, S., Gotoh, J., Takashi, M., "Experimental Analysis of Rolling Contact Stresses in a Viscoelastic Strip", Experimental Mechanics, Vol. 40, No. 2, p.p. 203–210, 2000. ■

N